ELSEVIER

Since January 2020 Elsevier has created a COVID-19 resource centre with free information in English and Mandarin on the novel coronavirus COVID-19. The COVID-19 resource centre is hosted on Elsevier Connect, the company's public news and information website.

Elsevier hereby grants permission to make all its COVID-19-related research that is available on the COVID-19 resource centre - including this research content - immediately available in PubMed Central and other publicly funded repositories, such as the WHO COVID database with rights for unrestricted research re-use and analyses in any form or by any means with acknowledgement of the original source. These permissions are granted for free by Elsevier for as long as the COVID-19 resource centre remains active.
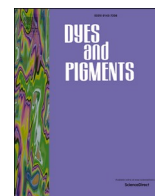
Short communication

Potent inhibition of Severe Acute Respiratory Syndrome Coronavirus 2 by photosensitizers compounds

Shujuan Yu [a], Gaohui Sun [a], Yaqun Sui [a], Hanlin Li [a], Yuhan Mai [a], Guodong Wang [a], Ning Zhang [b], Yuhai Bi [b,c], George F. Gao [b,c], Peng Xu [d], Longguang Jiang [a], Cai Yuan [d,***], Yang Yang [e,**], Mingdong Huang [a,*]

[a] College of Chemistry, Fuzhou University, Fujian, 350108, China
[b] CAS Key Laboratory of Pathogenic Microbiology and Immunology, Institute of Microbiology, Center for Influenza Research and Early-warning (CASCIRE), CAS-TWAS Center of Excellence for Emerging Infectious Diseases (CEEID), Chinese Academy of Sciences, Beijing, 100101, China
[c] University of Chinese Academy of Sciences, Beijing, 101408, China
[d] College of Biological Science and Engineering, Fuzhou University, Fuzhou, Fujian, 350108, China
[e] Shenzhen Key Laboratory of Pathogen and Immunity, National Clinical Research Center for Infectious Disease, State Key Discipline of Infectious Disease, Shenzhen Third People's Hospital, Second Hospital Affiliated to Southern University of Science and Technology, Shenzhen, China

ARTICLE INFO

ABSTRACT

The ongoing pandemic of coronavirus disease 2019 (COVID-19) posed a major challenge to the public health. Currently, no proven antiviral treatment for Severe Acute Respiratory Syndrome Coronavirus 2 (SARS-CoV-2) infection is available. Here we report compounds pentalysine β-carbonylphthalocyanine zinc (ZnPc5K) and chlorin e6 (ce6) potently inhibited the viral infection and replication in vitro with EC_{50} values at nanomolar level. These compounds were first identified by screening a panel of photosensitizers for photodynamic viral inactivation. Such viral inactivation strategy is implementable, and has unique advantages, including resistance to virus mutations, affordability compared to the monoclonal antibodies, and lack of long-term toxicity.

1. Introduction

The pandemic of coronavirus disease 2019 (COVID-19) caused by SARS-CoV-2 has exploded since December 2019, and causes more than 3.0 million death with more than 143 million people infected as of April 21st, 2021 globally [1,2]. Angiotensin-converting enzyme 2 (ACE2), expressed in the lungs, arteries, heart, kidney, intestines, and nasal epithelium [3], has been shown to be the primary entry point targeted by the surface spike protein of SARS-CoV-2.

There is currently no proven treatment for SARS-CoV-2 infection. Here we report the potent inactivation of the virus and its infection to ACE2 overexpression cells by photodynamic method using a number of photosensitizers.

2. Results

2.1. Screening photosensitizers by SARS-CoV-2 pseudoviruses entry assay

Firstly, we established a pseudoviral entry assay. In this assay, the pseudovirus containing the spike (S) protein of SARS-CoV-2 and EGFP protein encapsulated on HIV viral capsid (Fig. S1A) efficiently infected the human ACE2 expressing 293T cells (ACE2-293T) but not the plain 293T cells (Fig. S1B), indicating that the observed infection was mediated by the molecular interaction between the spike and ACE2 proteins. The bright green fluorescence of EGFP intensity is proportional to amount of pseudoviruses added to ACE2-293T cells.

Then, we screened a number of phthalocyanine photosensitizers for their antiviral effects using the pseudoviral entry assay. The photosensitizers were mixed with the pseudoviruses at the indicated concentrations and illuminated with a light-emitting diode (LED) light source to a light dose of 0.48 J/cm², then the mixture was incubated with ACE2-

---

293T cells for 48 h, followed by image analysis on a high-content imager. We calculated the inhibitory potencies (Fig. 1A and Table S1) of these photosensitizers based on EGFP fluorescence signal. It appears that the structural flexibility of the periphery group is important for the antiviral potency (Table S1). One of the photosensitizers, ZnPc5K, was identified as the most potent photosensitizer with the half-maximal effective concentrations (EC_{50}) values of 6.2 nM, and the 90% effective concentrations (EC_{90}) values of 114 nM (Fig. 1A). We also used a porphyrin-type photosensitizer ce6 as control candidate, and identified ce6 to have EC_{50} and EC_{90} values of 177 nM and 515 nM, respectively (Fig. 1A). These two photosensitizers completely abolished the infection of the pseudoviruses to the host cells at doses of 1.0 μM with LED light illumination (Fig. 1A). Importantly, these two photosensitizers did not affect cell morphology at this concentration under the light illumination (Fig. S2A), and showed almost no phototoxicity to ACE2-293T cells at concentration up to 5 μM (Fig. 1B). As a control, the photosensitizers did not affect the infection under the otherwise identical condition in the absence of LED light illumination (Fig. S2B). Furthermore, we studied whether these two photosensitizers could inactivate the pseudoviruses inside the ACE2-293T cells. We incubated the pseudoviruses with the ACE2-293T cells and photosensitizers for 4 h to allow viral infection to the cells, followed by LED illumination (0.48 J/cm^2). The cells were allowed to continue to grow for 2 days, followed by image analysis on a high-content imager. The results showed that both photosensitizers reduced the green fluorescence signal of the cells in a dose dependent manner (Fig. 1C). For ZnPc5K, the pseudoviral fluorescence signal was reduced by ~40% at a dose of 740 nM, while only about 20% reduction of pseudoviral fluorescence signal for ce6 was observed. Moreover, both photosensitizers showed little toxicity to the infected host cells as detected by nucleus stain (Fig. S2C).

2.2. Inactivation SARS-CoV-2 live viruses by ZnPc5K and ce6

To further confirm the antiviral efficiency of the two compounds, we used live SARS-CoV-2 to test the antiviral activity. The photosensitizers were incubated with SARS-CoV-2 viruses, followed by LED light illumination (0.48 J/cm^2). The mixture was then allowed to infect the Vero cells for 2 days, and the inactivation rates were evaluated by quantification of viral copy numbers in the cell supernatant via quantitative RT-PCR (qRT-PCR) and further confirmed with immunofluorescence staining (Fig. 2A and B). ZnPc5K and ce6 efficiently inhibited the live virus with EC_{50} values of 60.2 nM and 132 nM, and EC_{90} values of 331 nM and 341 nM, respectively (Fig. 2A). Upon ZnPc5K or ce6 treatments with illumination, Vero cells were shown almost no phototoxicity at concentration up to 5 μM (Fig. 2C). Meanwhile, photosensitizers had no effect on SARS-CoV-2 viruses under the identical conditions without LED illumination (Fig. S3). Taken together, photosensitizers ZnPc5K or ce6 were promising candidates for SARS-CoV-2 inactivation, and ZnPc5K had more potency.

Mechanistically, the photosensitizers most likely use the singlet oxygen to damage virus capsid protein or RNA, which is the typical reactive oxygen species (ROS) found with phthalocyanine type photosensitizer and has long half-life in viral capsid. The key finding of this work is the low toxicity of photodynamic method to the infected host cells with high potency to inactivate SARS-CoV-2 within the host cells. Such specificity of photosensitizer is likely due to the detoxifying capability of the cells, but not the virus. The cells contain several enzymes like superoxide dismutase and catalase, which can remove the ROS generated by the photosensitizers, making them more resilient to the insults from photosensitizers.

Cytotoxicity was further studied on fibroblast (HELF cells), and ZnPc5K showed no phototoxicity at concentration up to 5 μM, while ce6 showed no phototoxicity at concentration up to 1 μM (Fig. S4).

3. Discussion

Here we demonstrate the inactivation of SARS-CoV-2 either outside or within the host cells without significant toxicity using photosensitizers. Among these photosensitizers, ZnPc5K showed highest antiviral efficacy while maintaining no toxicity to cells [4]. This photosensitizer has low toxicity (acute oral toxicity > 5000 mg/kg) with no irritation to eyes or skins, and causes no mutagenesis to cells [5]. It has been demonstrated to be effective in antibacterial and anti-tumor cells in many studies. Generally, phthalocyanine type compound is quite safe and has been used as a color dye for outfits and underwear in fabric industry for over a century. Phthalocyanine type compound has also been used as an anti-tumor drug (Photosense®) for cancer treatment in Ukraine since 1990s [6]. Another phthalocyanine-based compound (Photocyanine®) is currently under Phase II clinical trial for esophagus cancer with a dose of 0.05–0.1 mg/kg in China [7,8]. Its Phase I trial demonstrated no major adverse effect in human at a dose of 2 mg/kg. Phthalocyanine green has been approved by FDA [9] to use in contact lens, surgical suture, and latex condom as a color additive. Phthalocyanine was also approved by FDA as Indirect Additives used in food contact substances. A surprised finding from this work is the high potency of ZnPc5K to inactivate virus with an EC_{50} of 60.2 nM, much higher than the typical micromolar range potencies for antimicrobial or antitumor applications of photosensitizers [10–12]. A number of studies found that photosensitizer-like structure with large ring-like organic compound, including methylene blue [13] and heme [14,15], may have specific binding to SARS-CoV-2 virus [16].

Photosensitizer requires light illumination to be effective for virus inactivation How to deliver light? There a couple scenarios for the applications of photosensitizers to inactivate virus [13,16,17]: (1) The SARS-CoV-2 virus entry receptors (ACE2 and TMPRSS2) are highly expressed in the nasal epithelium [3], and the virus was found to propagate in the upper respiratory tract, especially in the nose and oropharynx. The photodynamic treatment can reduce the number of virus present in the upper respiratory tract. Photosensitizer can be delivered directly by nebulization, following by LED light illumination. (2) The red light can be delivered through endoscope into the lung, which is relatively transparent to red light compared to other organs. In combination with photosensitizer, infused through vein, virus inside the lung can be inactivated, helping to reduce the burden of immune system. Such invasive procedure can be used in intensive care unit. As reported recently, systemic human neutralizing antibodies (HuNAbs) or vaccine failed full SARS-CoV-2 infection prevention in nasal turbinate and even post-exposure HuNAb suppressed SARS-CoV-2 in lungs but poorly in nasal turbinate. This study also reported that live SARS-CoV-2 persisted in nasal turbinate for several days despite systemic administration of human neutralizing antibodies (HuNAbs) that suppressed SARS-CoV-2 in lungs [18]. The monoclonal antibody HuNAbs or vaccine failed the full prevention of SARS-CoV-2 infection in nasal turbinate, which raised serious concerns [18]. It appears that PDT is one of the most promising method to intercept SARS-CoV-2 infection in nasal turbinate.

The current method of virus inactivation in our study has several advantages. First, this method works independent of viral sequences, and resistant to virus mutations. Photosensitizers use ROS to damage viral envelope proteins and/or nucleic acids. Such mechanism is most likely not sensitive to the mutations of SARS-CoV-2, which has been reported, e.g., D614G of the spike protein [19]. Second, the debris or the fragments generated from the virus by ROS could stimulate host immune defense. Third, photodynamic method to inactivate virus can be more affordable than other therapeutics like monoclonal antibody, which can be an important factor for preventive use at home. Other advantages of photodynamic inactivation include the lack of long-term toxicity, the ability to remove virus in a very short time, less damage to adjacent tissues, and high repeatability without viral resistance.

In summary, we demonstrated the high potencies (nM of EC_{50}) of photosensitizers in the inactivation of SARS-CoV-2 virus. Importantly,
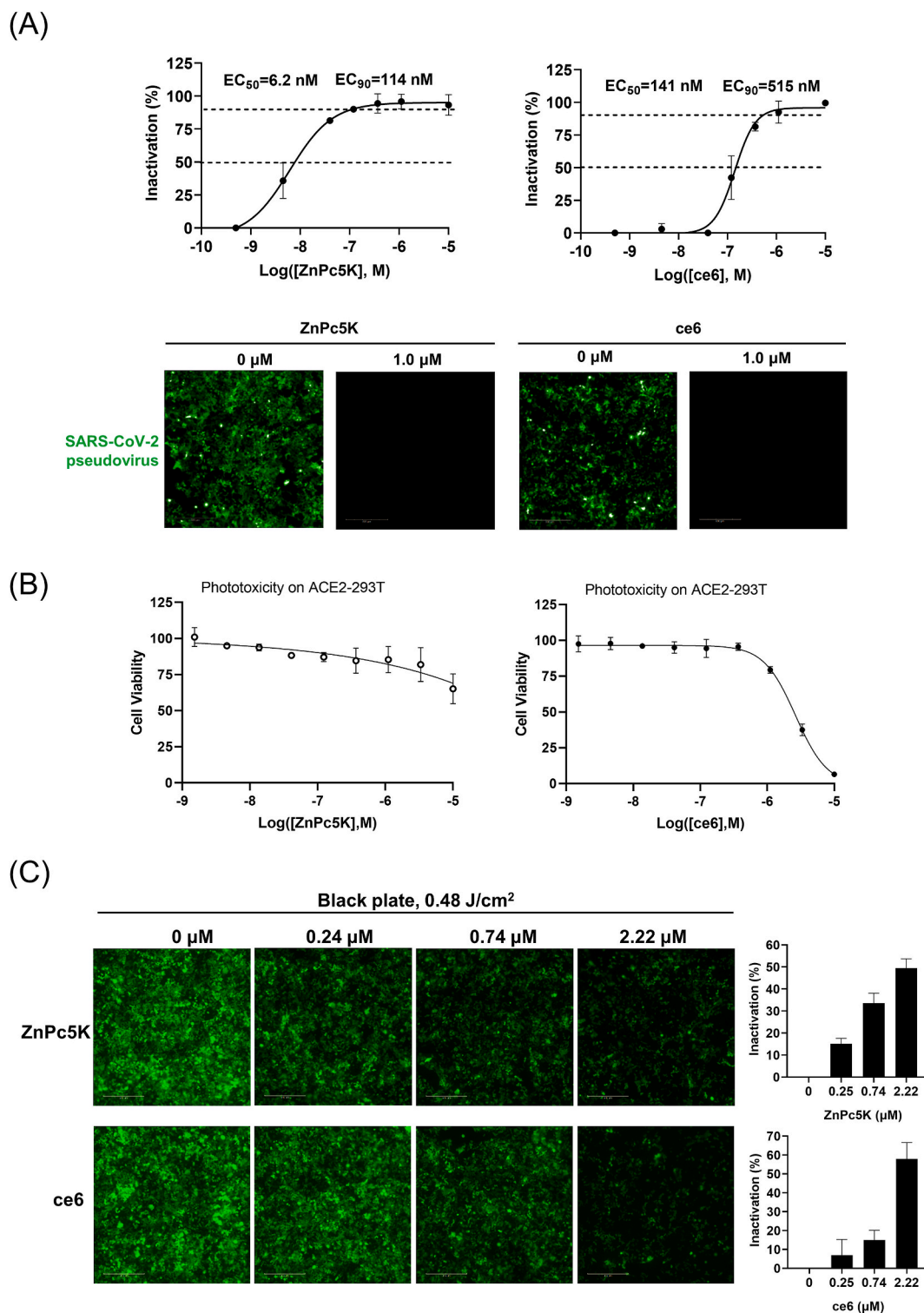
Fig. 1. Screening of two photosensitizers by SARS-CoV-2 pseudoviruses entry assay. (A) Dose-responses of the inhibition of viral infectivity were also measured for photosensitizer ZnPc5K and ce6, giving the EC$_{50}$ and EC$_{90}$. The photosensitizers completely inhibited the viral infectivity at 1 μM concentration upon LED illumination. The EGFP intensities of all fields in a microplate well at different concentrations were summed to represent the virus infected into the cells. Error bars represent the SD of duplicates in one experiment. Scale bar, 500 μm. (B) Photocytotoxicity of ZnPc5k and ce6 on hACE2-293T cells was measured by CCK-8 assay and showed almost no phototoxicity up to 5 μM with a light dose of 0.48 J/cm^2. (C) Photosensitizers inactivated the SARS-CoV-2 pseudoviruses and reduced virus load inside ACE2-293T cells upon LED illumination. Serially diluted ZnPc5K or ce6 and pseudoviruses were incubated with ACE2-293T cells for 4 h, and illuminated by LED to a light dose of 0.48 J/cm^2. After further 44 h incubation, the fluorescent images (green for EGFP for virus and blue for Hoechst for nucleus staining) were recorded and analyzed. Error bars represent the SD of triplicates in one experiment. Scale bar, 500 μm.
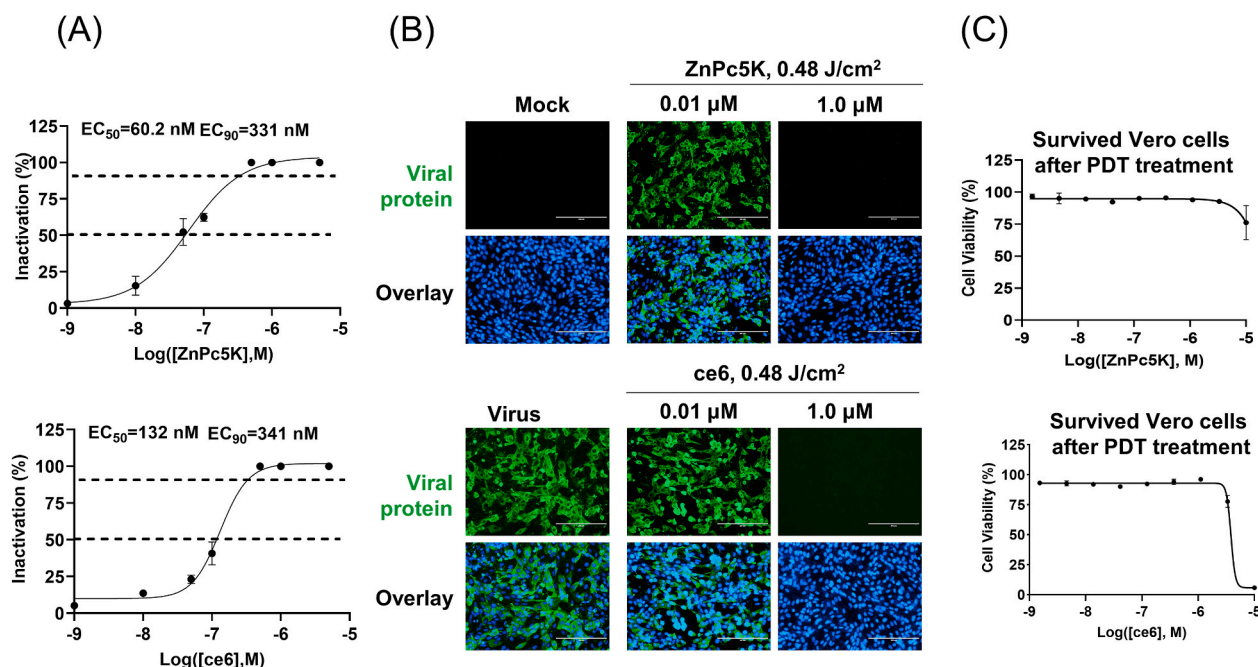
Fig. 2. Photosensitizers ZnPc5K and ce6 effectively inactivated SARS-CoV-2 live virus upon LED illumination. (A) Dose response curve of viral inactivation upon photodynamic treatment. The SARS-CoV-2 with a dose of 0.02 multiplicity of infection (MOI) was incubated with serially diluted photosensitizer and illuminated, followed by addition to Vero cells and further incubation for 48 h. The viral yield in the cell supernatant was quantified by qRT-PCR. (B) Immunofluorescence microscopic images of virus infection upon treatment of ZnPc5K and ce6 at the indicated concentrations with illumination showed the efficacy of photosensitizers to virus and safety to host cells. The fluorescence images were taken at 48 h post infection (h.p.i). Scale bar, 200 μm. Cells were stained with the viral protein (green) and nuclei (blue). (C) Cytotoxicity of ZnPc5K or ce6 to Vero cells was measured by CCK-8 assay and showed almost no phototoxicity up to 5 μM with a light dose of 0.48 J/cm^2.

the method can also reduce the virus load inside the human host cells with a large safety margin to cells.

4. Materials and methods

4.1. Chemicals and reagents

ZnPc5K was synthesized accordingly to our previously published procedure [20] (Fig. S5 and S6), which was also used to synthesize the compounds L1, L2, L4, L6, W2, W2A and W3 (Fig. S7). ce6 was from Cayman Chemical. Polybrene was from Sigma-Aldrich, USA. Puromycin was from Invitrogen, USA. Oligo nucleotides were synthesized by Sangon Biotech, China.

4.2. Cells and viruses

293T and Vero cells negative for mycoplasma were obtained from ATCC and cultured at 37 °C with 5% CO$_2$ in Dulbecco's Modified Eagle medium (DMEM) supplemented with 10% FBS (Gibco) and 1x penicillin-streptomycin (Invitrogen). SARS-CoV-2 pseudoviruses were purchased from Genewiz, China. SARS-CoV-2 strain BetaCoV/Shenzhen/SZTH-003/2020 (GISAID No. EPI_ISL_406594) was isolated and stored in the bio-safety level 3 laboratory in Shenzhen Third People's Hospital.

4.3. Lentivirus packaging and stable cell line construction

The pLVX-hACE2 plasmid was constructed by cloning the coding region from Human ACE2 cDNA ORF Clone with N-terminal Flag tag (SinoBiological, HG10108-NF, China) into pLVX-IRES-Puro Lentiviral vector between *Xho*I and *Not*I sites.

Lentivirus was packaged by co-transfection of pLVX-hACE2 or empty vector, with a mixture of VSV-G (Addgene, 8454), PRRE (Addgene, 12251) and REV (Addgene, 12253) plasmids by FuGENE (Promega) into

293T cells. The transfected medium was changed into fresh DMEM 8 h later. After 48 h of transfection, the lentivirus-containing supernatants were collected and filtered through a 0.45-μm filter, and diluted 1:1 with fresh medium containing 8 μg/mL polybrene, and were used to infect the target cells (293T) grown at 70–80% confluence. The selection antibiotic puromycin was added at a killing concentration 1–2 μg/mL to select cell line stably expressing ACE2. Fresh media with antibiotic were added every two days until all the cells in the control wells were dead.

4.4. Infection assay of SARS-CoV-2 pseudoviruses

Either plain 293T cells or ACE2-293T cells (4000 per well) were seeded in CellCarrier-384-well microplate (PerkinElmer) on day 0. SARS-CoV-2 pseudoviruses (0.4 × 10^5, i.e. MOI = 10) were then added to the cells on day 1. From then on, EGFP and bright field images of these wells were taken by Operetta High Content Imaging System every 24 h till day 8.

4.5. Inactivation assay of SARS-CoV-2 pseudoviruses by photosensitizers

Pseudoviruses inactivation assay was performed by mixture of SARS-CoV-2 pseudoviruses with serially diluted photosensitizers (such as ZnPc5K and ce6) with or without the light exposure using a LED light source (SunDynamic, Inc., Qingdao, 4 mW/cm^2) of 660 nm for 2 min (to a light dosage of 0.48 J/cm^2), followed by addition of the mixture into ACE2-293T cells. At 48 h post infection (h.p.i), the fluorescence images were taken and analyzed on Operetta High Content Imaging System (PerkinElmer). The relative viral infectivity was proportional to the sum of EGFP spot intensity on the cells and was analyzed by Operetta CLS software. Standard errors were estimated based on duplicates of the experiments.

Pseudoviruses cellular inactivation assay was carried out by mixing SARS-CoV-2 pseudoviruses with serially diluted photosensitizers. The mixture was added into ACE2-293T cells, and 4 h later illuminated by

LED with a power of 4 mW/cm^2 for 2 min. After incubation in CO_2 incubator for 48 h, images (EGFP for virus and Hoechst33342 for nucleus stain) were taken by Operetta High Content Imaging System to detect EGFP intensity.

An automated analysis method was used based on Operetta CLS™ System. To measure bioactivity of SARS-CoV-2 pseudoviruses, we calculated the sum of EGFP fluorescent intensity for pseudoviruses extracellular inactivation assay and the mean of EGFP fluorescent intensity for pseudoviruses cellular inactivation assay. For such analysis, we first defined nucleus with Hoechst-staining images, then cytoplasm with bright field images, and finally calculated the EGFP fluorescent intensity by going through all EGFP spots inside cells. The virus inactivation percentage was calculated by subtracting the intensity of EGFP of each group from the control of no photosensitizer, and divided by the control fluorescence. Error bars represent the SD of triplicates in one experiment.

4.6. Evaluation of antiviral activities of the photosensitizers using the live viruses

Firstly, the titer of the viral stock was measured by 50% tissue culture infective dose ($TCID_{50}$), then the antiviral activities of the photosensitizers were evaluated as previously reported with some modifications [21]. Vero cells were seeded in a 24-well transparent plate 24 h before infection. On the day of infection, the cells were washed twice with PBS. The SARS-COV-2 with a dose of 0.02 multiplicity of infection (MOI) was mixed with serially diluted photosensitizer (at the concentration of 0.001 μM, 0.01 μM, 0.05 μM, 0.1 μM, 0.5 μM, 1 μM or 5 μM) in cell culture medium without or with the light exposure using a LED light source of 660 nm and with a power of 0.48 J/cm^2. This mixture (500 μL) was added to the Vero cells and further cultured with fresh DMEM with 2% FBS at 37 °C. At 48th h.p.i, the cell supernatant was collected and viral RNAs were extracted using the QIAamp RNA Viral Kit (Qiagen, Heiden, Germany) for further quantification analysis. The cells were collected for immunofluorescence assay. All the experiments involving infectious SARS-CoV-2 were handled in BSL-3 facilities at the Shenzhen Third People's Hospital.

4.7. Quantitative real-time PCR

Viral RNAs were extracted from the samples using the QIAamp RNA Viral Kit (Qiagen, Heiden, Germany), and qRT-PCR was performed using a commercial kit (Genrui-bio) targeting the S and N genes [22]. The specimens were considered positive if the Ct value was less than 38.0, and negative if the results were undetermined. Specimens with a Ct higher than 38 were repeated. The specimen was considered positive if the repeat results were the same as the initial result and between 38 and 40. If the repeat Ct was undetectable, the specimen was considered negative.

4.8. Immunofluorescence assay

The procedure was similar to our previously published report [21]. Briefly, vero cells were fixed in 4% formaldehyde at 48th h.p.i. Then cells were permeabilized in 0.5% Triton X-100, blocked in 5% BSA in PBS, and then probed with the plasma of this patient or healthy control at a dilution of 1:500 for 1 h at room temperature. The cells were washed three times with PBS and then incubated with either goat anti-human IgG conjugated with Alexa fluor 488 at a dilution of 1:500 for 1 h (Invitrogen). The cells were then washed and stained with Hoechst33342 (Invitrogen) to detect nuclei. Fluorescence images were obtained and analyzed using EVOS FL Auto Imaging System (Invitrogen).

4.9. CCK-8 assay

The cell viability/cytotoxicity was measured by Cell Counting Kit-8 (CCK-8) (Meilunbio). Briefly, the cells were seeded in ViewPlate-96-well plate (PerkinElmer), and treated with serially diluted photosensitizers, followed by LED illumination with a power of 4 mW/cm^2 for 2 min at 4 h later. After incubation in CO2 incubator for 24 h, 10 μl of CCK-8 solution was added to each well, and the 96-well plate was incubated at 37 °C for 1 h. Normal DMEM with CCK-8 solution and the cells with no photosensitizer served as the blank control and normal control, respectively. The cell viability was calculated according to the product manufacturer's instructions using the OD450nm measured on a microplate reader (SpectraMax® i3x, Molecular Devices). All doses were done at triplicates.

CRediT authorship contribution statement

Shujuan Yu: Data curation, Formal analysis, Design of experiments, execution and data analysis. **Gaohui Sun:** partial initial screening. **Yaqun Sui:** partial initial screening. **Hanlin Li:** ACE2 plasmid construction. **Yuhan Mai:** organic synthesis (L1, L2, L3 and L4). **Guodong Wang:** organic synthesis (W2, W2A and W3). **Ning Zhang:** Data curation, data of live SARS-CoV-2 data. **Yuhai Bi:** Resources, manuscript revision. **George F. Gao:** Resources, manuscript revision. **Peng Xu:** manuscript revision. **Longguang Jiang:** manuscript revision. **Cai Yuan:** manuscript revision, Supervision, Resources, Writing – review & editing, Funding acquisition. **Yang Yang:** measurements of live SARS-CoV-2 data, data interpretation, manuscript revision, Resources. **Mingdong Huang:** Supervision, Resources, Writing – review & editing, manuscript submission, Funding acquisition.

Declaration of competing interest

The authors declare that they have no known competing financial interests or personal relationships that could have appeared to influence the work reported in this paper.

Acknowledgements

Appendix A. Supplementary data

Supplementary data to this article can be found online at https://doi.org/10.1016/j.dyepig.2021.109570.

References

[1] WHO coronavirus disease (COVID-19) dashboard. 2020.

[2] Wiersinga WJ, Rhodes A, Cheng AC, Peacock SJ, Prescott HC. Pathophysiology, transmission, diagnosis, and treatment of coronavirus disease 2019 (COVID-19): a review. J Am Med Assoc 2020;324:782–93.

[3] Sungnak W, Huang N, Bécavin C, Berg M, Queen R, Litvinukova M, et al. SARS-CoV-2 entry factors are highly expressed in nasal epithelial cells together with innate immune genes. Nat Med 2020;26:681–7.

[4] Li L, Luo Z, Chen Z, Chen J, Zhou S, Xu P, et al. Enhanced photodynamic efficacy of zinc phthalocyanine by conjugating to heptalysine. Bioconjugate Chem 2012;23:2168–72.

[5] Ying C, Hailin W, Fan Y, Xiaobei Q, Kening Y, Panpan C. Safety evaluation of an amino acid based photosensitizer (in Chinese). J Toxicol 2015;29:477–9.

[6] Smirnova ZS, Oborotova NA, Makarova OA, Orlova OL, Polozkova AP, Kubasova IY, et al. Efficiency and pharmacokinetics of photosense: a new liposomal photosensitizer formulation based on aluminum sulfophthalocyanine. Pharmaceut Chem J 2005;39:341–4.

[7] Chen D, Song M, Huang J, Chen N, Xue J, Huang M. Photocyanine: a novel and effective phthalocyanine-based photosensitizer for cancer treatment. J Innov Opt Health Sci 2020;13:2030009.

[8] Li S, Bi B, Luo G, Zhan J, Zhang R, Li J, et al. A phase I study to evaluate the application of photocyanine using pharmacokinetic and pharmacodynamic analysis in patients with malignancy. Canc Chemother Pharmacol 2020;86:267–76.

[9] Summary of color Additives for use in the United States in foods, drugs, cosmetics, and medical devices. 2020.

[10] Chen Z, Zhang Y, Wang D, Li L, Zhou S, Huang JH, et al. Photodynamic antimicrobial chemotherapy using zinc phthalocyanine derivatives in treatment of bacterial skin infection. J Biomed Opt 2016;21:18001.

[11] Chen Z, Zhou S, Chen J, Deng Y, Luo Z, Chen H, et al. Pentalysine beta-carbonylphthalocyanine zinc: an effective tumor-targeting photosensitizer for photodynamic therapy. ChemMedChem 2010;5:890–8.

[12] Chen Z, Zhou S, Chen J, Li L, Hu P, Chen S, et al. An effective zinc phthalocyanine derivative for photodynamic antimicrobial chemotherapy. J Lumin 2014;152: 103–7.

[13] Gendrot M, Andreani J, Duflot I, Boxberger M, Le Bideau M, Mosnier J, et al. Methylene blue inhibits replication of SARS-CoV-2 in vitro. Int J Antimicrob Agents 2020:106202.

[14] Liu W, Li H. Preprint at, https://doi.org/10.26434/.chemrxiv11938173v9; 2020.

[15] Read RJ. Preprint at, https://doi.org/10.26434/.chemrxiv12120912v1; 2020.

[16] Kipshidze N, Yeo N, Kipshidze N. Photodynamic therapy for COVID-19. Nat Photonics 2020;14:651–2.

[17] Dias LD, Blanco KC, Bagnato VS. COVID-19: beyond the virus. The use of photodynamic therapy for the treatment of infections in the respiratory tract. Photodiagnosis Photodyn Ther 2020;31:101804.

[18] Zhou D, Chan JF, Zhou B, Zhou R, Li S, Shan S, et al. Robust SARS-CoV-2 infection in nasal turbinates after treatment with systemic neutralizing antibodies. Cell Host Microbe 2021;29(4):551–63.

[19] Plante JA, Liu Y, Liu J, Xia H, Johnson BA, Lokugamage KG, et al. Spike mutation D614G alters SARS-CoV-2 fitness. Nature 2021;592:116–21.

[20] Chen J, Chen H, Li Y, Wang J, Chen N, Huang J, et al. Synthesis and photodynamic activity of a new type of pentalysine 2-carbonylphthalocyanine zinc (in Chinese). Chem J Chin Univ 2008;29:2131–7.

[21] Zhang H, Yang Y, Li J, Wang M, Saravanan KM, Wei J, et al. A novel virtual screening procedure identifies Pralatrexate as inhibitor of SARS-CoV-2 RdRp and it reduces viral replication in vitro. PLoS Comput Biol 2020;16:e1008489.

[22] Zhao F, Yang Y, Wang Z, Li L, Liu L, Liu Y. The time sequences of respiratory and rectal viral shedding in patients with coronavirus disease 2019. Gastroenterology 2020;159. 1158-60.e2.